Clinical Reviews in Bone and Mineral Metabolism (2019) 17:24–39
https://doi.org/10.1007/s12018-018-9255-y

REVIEW PAPER

Fourier Transform Infrared Spectroscopy of Bone Tissue: Bone Quality Assessment in Preclinical and Clinical Applications of Osteoporosis and Fragility Fracture

Nikolaos Kourkoumelis[1] · Xianzuo Zhang[2] · Zeming Lin[3] · Jian Wang[3]

Published online: 10 January 2019
© Springer Science+Business Media, LLC, part of Springer Nature 2019

Abstract

The pathogenesis of bone fragility is of utmost importance especially to modern societies with aging populations. Increased skeletal fragility due to aging and disease motivates researchers to investigate the contributing biological mechanisms and to find ways to inhibit them. Bone quality is a set of structural and compositional variables that contribute to bone strength and influence its ability to resist fracture. They originate from multiple bone hierarchical levels and include the morphology (mass distribution), the chemical composition, and the biomechanical properties of bone tissue such as stiffness, fatigue strength, and fracture toughness. Qualitative and quantitative measurements of bone material properties reflect the underlying health or disease status. Fourier transform infrared (FTIR) spectroscopy and imaging are able to evaluate spatially inhomogeneous structures like bone in the form of sections or homogenized powder, providing simultaneous quantitative and qualitative information from both organic and inorganic tissue components. These techniques give a snapshot of structural and material properties that essentially depend on bone turnover while they are also sensitive to tissue alterations due to metabolic and nonmetabolic diseases, and external factors like administration of drugs. In this review, we discuss the application of FTIR spectroscopy and imaging to preclinical and clinical studies. The interpretation of results emphasizes the potential of infrared spectroscopic techniques to associate bone heterogeneity with fracture risk, assess the compositional and structural properties of osteoporotic bone, and investigate bisphosphonates' antiresorptive action and side effects.

Keywords Fourier transform infrared spectroscopy · FTIR · Imaging · Bone quality · Osteoporosis · Fragility fracture · Bone molecular structure

Tissue diagnostics depends on clinical observations to identify the underlining conditions or determine their severity. Bone disorders are typically probed by imaging, serum biomarkers, and patient risk factors. For example, risk assessment guidelines [1] and X-ray radiation are the main clinical tools to evaluate those considered to be at risk of a first fragility fracture. However, the majority of individuals at high risk of fractures are neither diagnosed or treated for probable osteoporosis; moreover, the sensitivity of bone density imaging techniques cannot entirely identify individuals who will or will not develop fractures [2], conceivably because bone density mostly refers to bone quantity. Other examples of bone disorders, typically diagnosed with imaging techniques like radiography, dual-energy X-ray absorptiometry (DEXA), quantitative CT, and ultrasound, include osteomalacia, rickets, scurvy, renal osteodystrophy, hyperparathyroidism, Paget's disease, osteogenesis imperfecta, acromegaly, and osteopetrosis [3]. When common diagnostic procedures do not provide a clear answer as to what needs to be done to prevent a fracture, bone diagnostics turns to the ex vivo analysis of bone biopsies. Although invasive, this technique can assert the presence of

✉ Nikolaos Kourkoumelis
nkourkou@uoi.gr

[1] Department of Medical Physics, School of Health Sciences, University of Ioannina, 45110 Ioannina, Greece

[2] Department of Orthopedics, Anhui Provincial Hospital, University of Science and Technology of China, Hefei, Anhui, China

[3] Department of Arthroplasty, Nanfang Hospital, Southern Medical University, Guangzhou, Guangdong Province, China

malignant cells, the paucity of bone cells, and abnormal mineralization through histology and histomorphometry.

Fourier transform infrared (FTIR) spectroscopy is a vibrational spectroscopic technique able to detect the subtle changes attributed to the way that pathological tissues function [4]. It has the potential to aid bone diagnostics, as a method that assists the histomorphometric analysis or as an automated process for histopathology classification [5]. In essence, it relies on the principle that molecular bonds absorb specific electromagnetic frequencies which are dependent on their chemical nature. However, contrary to conventional histological analysis, FTIR does not require specific staining (label-free method) and is able to rapidly probe many key (bio)molecules simultaneously measuring spatial alterations in bone composition with high chemical specificity. Furthermore, bone strength and toughness depend on nucleation and progression of cracks and consequently, on microscopic material defects like fiber organization and inorganic/organic interfaces and properties [6] which can be readily assessed by FTIR. With this approach, it is possible to introduce new bone biomarkers and investigate biophysical mechanisms related to a disease since the method exhibits increased sensitivity in discriminating normal from diseased tissues or effective from less effective therapeuticals. These advantages are attributed to the fact that FTIR spectroscopy can simultaneously probe the chemical composition of biological samples as well as the corresponding biomolecular interactions. As FTIR shows increased sensitivity to the unique parameters of each measured sample, the obtained spectra are commonly described as molecular fingerprints.

Here, we review the application of FTIR spectroscopy to preclinical and clinical studies, emphasizing its potential to aid the unbiased clinical decision and enhance our knowledge regarding normal and diseased bone tissue function and metabolism.

Bone Molecular Structure

Bone is a heterogeneous, hierarchically structured, composite material which essentially consists of calcium phosphate crystals periodically deposited on soft organic matter (mainly type I collagen). These so-called mineralized collagen fibrils are being formed during the bone biomineralization process [7]. Bone heterogeneity is due to the continuous process of bone resorption and formation (remodeling) while its hierarchical structure comprises of several structural levels from macro to nanometer scale [8]. Both structure and heterogeneity contribute to the excellent mechanical properties of healthy bone which can be summarized to high stiffness, strength, toughness, and lightweight structure [9]. At the molecular level, where FTIR spectroscopy exerts its analytical power, we can distinguish the components of inorganic mineral and organic matrix. The inorganic mineral phase is poorly crystalline, calcium-deficient, carbonated hydroxyapatite (HA), $[Ca_{10}(PO_4)_6(OH)_2]$, with several impurities such as HPO_4^{2-}, CO_3^{2-}, Mg^{2+}, Na^+, F^-, and citrate [10] which are adsorbed onto the mineral surface and are substituted in the lattice for Ca^{2+}, PO_4^{3-}, and OH^- ions [11]. Bone maturation causes an increase in mineral crystal size and perfection due to changes in ionic substitutions and chemical stoichiometry. Absorption and dissolution is achieved by controlling the rate of cationic and/or anionic substitutions [12]. Hence, bone homeostasis and adaptation largely depends on increased mineral solubility which is enhanced by the nonstoichiometric apatite structure which in turn is imposed by compositional impurities [13] and the small size of the apatite nanocrystals [14]. With aging, mature apatite becomes more stoichiometric while the average crystallites size increases on top of crystallinity. On the other hand, mineral content and grain size both contribute to bone strength since, with insufficient mineralization, bones would plastically deform under load and there is an apparent relationship between the size of mineral grains and the elastic modulus of the bone matrix [15, 16]. Furthermore, studies in animals (tibias of female BALB mice harvested between 1 and 40 days of age) with FTIR microspectroscopy correlated with morphometric (μCT), and mechanical (nanoindentation) analyses showed that bone stiffness is affected by both mineral content (tissue density) and tissue composition (measured by FTIR). Specifically, using a generalized linear model for the FTIR measurements, the elastic modulus was determined by the level of mineralization and collagen cross-linking when all the other chemical parameters we considered as covariates [17].

Collagen type I is the predominant biomolecule (90%) in the organic matrix and provides the necessary toughness to bone to resist fracture. It is a fibrous protein with three left-handed α-like polypeptide chains, and it is synthesized by osteoblasts to a right-handed triple-helical structure. It consists of [Gly-X-Y]n sequences where X and Y are proline and hydroxyproline [18]. Enzymatic and nonenzymatic cross-linking provides the fibrillar matrix with tensile strength and viscoelasticity [19]. The rest of the organic phase in the extracellular bone are mainly noncollagenous proteins. Almost 75% of the about 200 noncollagenous proteins are synthesized by osteoblasts while the rest are deposited in the bone matrix by serum [20]. Although in low concentration, they are important for bone remodeling initiating mineralization [21–23].

FTIR spectroscopy is able to explore both inorganic and organic phase alterations in one go. Typical outcomes which reflect bone condition are: level of mineralization, mineral maturity, carbonate accumulation and environment, acid phosphate content, and collagen cross-linking [24]. The impact of these parameters on bone failure are not necessarily equally reflected on the mechanical properties of bone tissue.

Yet, FTIR can suggest predictors of fracture risk which are of clinical importance and provide diagnostic information on diseases that disrupt the bone matrix or the mineralization process.

Bone Quality

There is a wide variety of experimental methods for assessing bone health status [25]. Their applicability ranges from the molecular to macro-scale, and their target are the geometric, compositional, and mechanical bone properties. In a clinical setting, the main focus is towards evaluating bone mass, i.e., the amount of mineralized bone material in a given volume. The measurement of bone mineral density (BMD) is currently the most commonly used densitometric technique for quantifying bone fracture risk. Bone mineral content depends on peak bone density achieved during development and subsequent bone loss; hence, low BMD can result from deficient bone accretion, accelerated bone loss, or both [26]. Areal bone mineral density (aBMD, i.e., bone mass along the X-ray projection) is usually assessed by DEXA and it is currently the gold standard for fracture risk prediction conveyed as T-scores [27]. Specifically for fragility, defined as fracture susceptibility, the Rotterdam study [28] suggested that densitometric measurements alone, i.e., T-score < −2.5, are not sufficient to predict almost half of nonvertebral fractures in postmenopausal women. As a result, the term of "bone quality" emerged to address diagnostic ambiguities in BMD scores of individuals who do and do not sustain osteoporotic fractures. Even so, this description has the disadvantage of being dependent on the limitations of a clinical technique, and therefore, it is not considered as self-sufficient [29]. Generally, bone quality accounts for bone structural and compositional variables such as the spatial distribution of the bone mass and the inherent/interacting properties of the molecular groups of the bone tissue [30]. Although the biochemical and biophysical factors that are collectively known as "bone quality" cannot be precisely defined, they are usually named as "intrinsic determinants" and include collagen-mineral composition, collagen characteristics, ultrastructural morphology, cellular activity, microdamage, and fatigue [31, 32].

In the next sections, we will provide a brief theoretical background for FTIR spectroscopy, the intrinsic determinants that can be evaluated, and some recent preclinical and clinical applications that enhance established diagnostic procedures like BMD and histomorphometry.

Short Introduction to FTIR Spectroscopy

Molecular spectroscopy relies on the quantum physics phenomenon that a photon undergoes absorption, emission, or scattering by a molecule, when a change in the energy of a molecule occurs. In particular, infrared spectroscopy probes vibrations of molecular bonds when infrared radiation passes through a sample mass [33]. Molecules have discreet energy levels for electronic transitions, molecular vibrations, and molecular rotations. When a molecule is irradiated by monochromatic light, it absorbs a fraction of the incident radiation at a specific energy, and undergoes transition from a lower (usually referred as ground level) to a higher energy state (denoted as excited level). These levels must be separated by exactly the same energy difference. Moreover, there are selection rules imposed by quantum mechanics and group theory which distinct transitions as allowed and forbidden. For infrared spectroscopy the key selection rule is that the electric dipole moment of the molecule must change during the vibration; consequently, the peak intensity increases with increasing polarity. In summary, the peaks in an FTIR spectrum are due to the transitions between quantized energy levels of molecular vibrations and correspond to the frequency of bond vibration of a molecule. These vibrations are localized to specific moieties of a molecule called functional groups. The position of an infrared absorption band (usually in wavenumber units, cm^{-1}) is affected by the vibrating masses, the type of molecular bond, the electron withdrawing or donating effects of the intra- and intermolecular environment, and the coupling with other vibrations [34] and reveal the vibrational energy levels of the functional groups present in a molecule. Infrared spectra peaks are eventually assigned to the specific vibrations of the corresponding functional groups, and consequently, the derived spectrum is a superposition of all of the constituents of the measured sample offering a wealth of biodiagnostic information. Different functional groups have different peak intensities, peak widths, and typically different positions (i.e., quantitatively absorb in different infrared regions), providing a chemical sensitive profile of the specimen, hence the term "molecular fingerprinting." Within small variations, each peak position denote specific species, the peak height is proportional to the concentration of certain chemical moieties, and the peak width gives an estimate of intermolecular interactions (i.e., broad peaks correspond to strong interactions).

Apart from the conventional FTIR spectroscopy, FTIR imaging provides spatially resolved information based on multiple IR spectra in an array format. In an FTIR image, every pixel comprises an entire spectrum that provides a biochemical fingerprint of the measured sample which can be then analyzed for disease status or type classification. FTIR spectroscopic imaging has the advantage of being a fast and label-free imaging technology (fixation can be also used), has high chemical specificity, and provides spatial information of the chemical components of a specimen, and the representative IR images are generated in a single measurement of the sampling area. FTIR spectroscopy and imaging applied to biological systems are

typically performed in three configurations: reflection, transmission, and attenuated total reflectance (or "reflection," ATR) [35, 36], although FTIR spectra can be also acquired with other modalities like polarized FTIR imaging and photoacoustic infrared spectroscopy [37]. A drawback in using FTIR spectroscopy for the assessment of tissue quality is the intense absorbance of water in the infrared. Therefore, dehydration is normally a prerequisite. Moreover, when FTIR is used in transmission mode, samples must be homogenized with KBr and pressed into thin pellets. Finally, tissue fixation and microtoming of thin sections are typically required for imaging [25]. ATR-FTIR spectroscopy requires minimal sample preparation (along with other advantages like in situ measurements, minimal water interference, and increased spatial resolution for imaging [38]) and has been recently employed for the quantification of bone mineral crystallinity [39]. Likewise, ATR-FTIR has been used in forensics to investigate how different exposure times are able to predict burning temperatures of bone. Using multivariate linear regression analysis, the splitting of the v_4 PO_4 domain was used to determine the crystallinity index of burnt bone [40]. Nevertheless, ATR-FTIR has not been extensively used in the bone field possibly due to the small light penetration depth which makes the technique ideal for highly absorbing samples and thin surfaces. Conversely, thick samples can cause saturation effects; furthermore, some contact pressure is necessary on samples to the ATR crystal [38]. Photoacoustic infrared spectroscopy was used to study undisturbed human cortical bone [41]. It was found that the photoacoustic mode is more sensitive to specific amide and carbonate bands than transmission mode. Furthermore, it provides depth profiling analysis and requires little to no sample preparation.

As the principle behind image acquisition is still the interaction of infrared light with the vibrational modes of the infrared (IR) active molecules, the instrumentation details of the various FTIR (micro) spectroscopy and imaging techniques will not be discussed here. A recent review on articular cartilage and osteoarthritis studies by FTIR imaging gives an in-depth explanation of the different FITR imaging modalities [42]. In the subsequent sections, we will use the term spectroscopy and imaging where appropriate and the results can be directly compared because they refer to the same parameters of bone physiology.

Bone FTIR Band Assignment

The building blocks of bone matrix are the inorganic component of hydroxyapatite crystals and the organic component, osteoid. Both have specific chemical signatures and, consequently, distinctive infrared spectra with structure-sensitive features (Fig. 1). The major FTIR bands for bone tissue and their assignments are summarized in Table 1.

Figure 1 shows that FTIR bone spectra can be roughly separated into two regions where the organic and inorganic components have distinct peaks. The intense band at 1654 cm^{-1} is attributed to amide I (peptide C=O stretching vibration of the collagen) while near 1550 cm^{-1} a combination of the C–N stretch and N–H in-plane bending modes are assigned to amide II functional group. The strong absorption contour at 900–1200 cm^{-1} is attributed to the v_1 and v_3 normal modes of the apatitic phosphate ion of hydroxyapatite. The free phosphate ion can have four modes of vibrations: v_1 (A_1) (symmetric stretching), v_2 (E) (symmetric bending), v_3 (T_2) (antisymmetric stretching), and v_4 (T_2) (antisymmetric bending) [44]. Due tetrahedral symmetry (T_d), only the v_3, v_4 vibration modes are FTIR active; however, the additional v_1, v_2 modes can be observed when the molecule organizes itself to lower symmetry. In bone FTIR spectra, these interactions result in the weak bands at 957 cm^{-1} and 473 cm^{-1}. The v_4 bending mode is triply degenerate but due to local anisotropic crystal field effects, it appears as a well-defined doublet at 563 and 604 cm^{-1}. The band at 1163 cm^{-1} is attributed to the HPO_4^{2-} which is related to nonstoichiometric hydroxyapatite and to the content of organic matter [45]. It is expected to decrease with age because as the concentration of carbonate ions increases during apatite maturation, the amount of labile HPO_4^{2-} decreases, keeping the Ca/(C+P) atomic ratio almost constant [46, 47]. The carbonate concentration is also age dependent. The free ion adopts D_{3h} molecular symmetry (planar–trigonal geometry with one atom at the center and three atoms at the corners of an equilateral triangle) with four vibration modes v_1 (A_1') (symmetric stretching), v_2 (A_2") (out of plane bending), and two doubly degenerate v_3, v_4 (E') of which only the last three are infrared active. However, the v_1 band is allowed when the structure shifts to lower symmetry. The ion occupies three different sites in biological hydroxyapatite: in monovalent anionic sites substituting for the hydroxyl group (A-type), in trivalent anionic sites substituting for the phosphate group (B-type), and on the surface of bone apatite at random locations (labile). The exact occupancy and location of the carbonate ions in the lattice are evasive due to the nanodimensions of the apatite crystallites. Studies with neutron and X-ray powder diffraction have showed that CO_3^{2-} ions replace PO_4^{3-} ions in the lattice by either occupying the mirror symmetry-related faces of the vacated PO_4 site or the adjacent faces of a PO_4 tetrahedron parallel to the c crystallographic axis [48, 49]. The CO_3^{2-} v_3 (1456 cm^{-1}) band overlaps with the intense absorption bands of organic material while the v_4 is a very weak band at 669 cm^{-1}. Thus, the v_2 mode is preferable for quantitative calculations of carbonates in bone mineral.

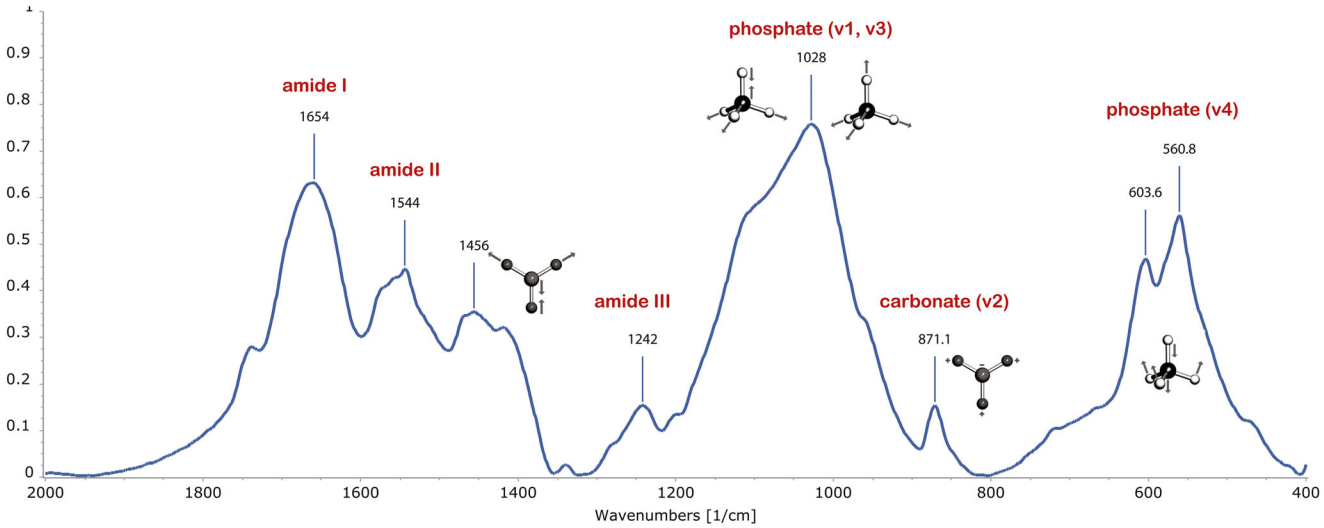

Fig. 1 Typical FTIR spectra of rabbit femur (cortical section). The normal modes of the phosphate (T_d symmetry) and carbonate (D_{3h} symmetry) ions are shown along with the amide bands

Bone FTIR Structural and Compositional Information

Qualitative and quantitative information from the complex bone organization can be extracted by FTIR spectra analysis through a series of mathematical procedures, categorized as pre- and postprocessing [50, 51]. Preprocessing is a set of resolution enhancement tasks to better resolve the absorption bands and minimize noise. This challenging process improves the robustness of any subsequent quantitative or classification study [52]. Postprocessing involves the application of multivariate analysis for dimensionality reduction, data classification, detection of trends, and removal of outliers [53, 54]. Still, no universal procedures and algorithmic tools exist for the processing and interpretation of IR spectra and images.

Bone FTIR spectra feature wide composite bands which enclose multiple underlying peaks attributed to bonds vibrational modes and neighboring atom interactions. To decipher compositional features hidden by stronger signals, second-derivative spectroscopy is often applied for accessing the exact position of the underlying peaks (i.e., reducing the overlap between IR bands by decreasing their width-to-intensity ratio) [55] and Fourier self-deconvolution for evaluating the relative contribution of the vibrating functional groups [56]. Deconvolution of the v_4 normal mode of phosphate ions generates five sub-bands which give an estimate of the nonapatitic

Table 1 Tentative assignment of the most prominent bone FTIR bands [24, 43]

Assignment	IR frequency (cm^{-1})
PO_4^{3-} v_2	473 w
PO_4^{3-} v_4	563 s, 604 s[a], (575 sh)[b]
CO_3^{2-} v_4	669 w
CO_3^{2-} v_2	871 s[a]
PO_4^{3-} v_1	957 sh
PO_4^{3-} v_3	1028 s, 1101, (1065)[b]
HPO_4^{2-} v_3	1163 w
Amide III	1242 s
CH_2 wagging	1340 s
νCOO^-	1398 s
$\delta_{as}CH_3$, CO_3^{2-} v_3	1456 s[b]
$\nu_{as}COO^-$	1510[b]
Amide II δ(N–H) ν(C–N) (C–N stretching and N–H in-plane bending)	1542 s–1562 s
Amide I (peptide carbonyl group (–C=O) stretch)	1654 s

s strong intensity, *w* weak intensity, *sh* shoulder

[a] IR envelope

[b] Poorly resolved peaks

and acid phosphate content. Specifically, there are two bands near 621 cm^{-1} and 532 cm^{-1} which are attributed to nonapatitic and acid phosphate content, respectively. The fundamental PO_4^{3-} v_4 mode appears near at 561, 580, and 604 cm^{-1} and resembles the crystalline apatite content (Fig. 2). Carbonate content is defined by deconvolution of the CO_3^{2-} v_2 contour using three sub-bands located near 879, 871, and 866 cm^{-1}. The first two bands point to the apatitic locations of the carbonate ion in the two anionic sites of the structure, normally occupied by phosphate and hydroxyl ions, respectively. In this way, A-type vs. B-type apatite can be discriminated (Fig. 2). The significantly increased intensity of the B-type sub-band implies that biological apatites are mainly B-type carbonate apatites with small fractions of A-type impurities at a relatively constant ratio (approximately 15%) [57]. The third band is assigned to labile (i.e., nonapatitic) carbonate which decreases with age although the overall carbonate content increases. Table 2 summarizes the bone properties that can be assessed by FTIR spectroscopy and which can be summarized to mineral to matrix ratio, mineral maturity/crystallinity, carbonate to mineral ratio, carbonate accumulation, acid phosphate substitution, and type I collagen cross-link ratio. The overall analysis is based on the principle that in FTIR, peak ratios are proportional to the relative content of the corresponding species.

As it is evident from Table 2, there are two parameters (mineral maturity and collagen cross-links) that need further discussion. Mineral maturity is often used interchangeably with "crystallinity." The latter term is defined as the crystallite size/strain and perfection of bone crystallites, and it is typically assessed by X-ray diffraction line broadening analysis. It was suggested [68] that these features must be disengaged as two distinct properties of bone tissue, mostly because they are poorly correlated in studies with human bone specimens. However, through FTIR crystallinity can be assessed by full width at half maximum $(FWHM)^{-1}$ of the 604 cm^{-1} peak. Narrow peaks imply high crystallinity index. Both size and perfection of apatite crystals contribute to bone strength. Bala et al. [69] suggested that long-term (6–10 years) alendronate treatment of postmenopausal osteoporosis compromised the micromechanical properties (tissue-level modulus and hardness) of ex vivo cortical bone samples mainly due to a decrease in mineral crystallinity. The decrease in crystallinity under treatment was mainly attributed to a deficiency in the crystal perfection rather than in the size of crystals, caused by alendronate independently of its antiresorptive action.

Collagen cross-linking strongly affects the biological and biomechanical features of bone. Its toughness is largely dependent on the organic matrix when enzymatic cross-links stabilize the initial steps in collagen fibril formation and mineralization and supply the matrix with tensile strength and viscoelasticity [70, 71]. Intrinsic toughening (i.e., plasticity) stems from the sliding mechanism along the mineralized collagen fibrils [72]. Reducible enzymatic cross-links form a template for mineralization by stabilizing the early unmineralized fibril. With aging, irradiation, and certain diseases, these labile cross-links turn into a limited number of irreducible (or nonreducible) cross-links between fibrils at specific points of collagen molecule and impede the intrinsic toughening mechanism which is then accommodated by inelasticity due to microcracks [72]. Mature pyridinium collagen cross-links, pyridinoline and deoxypyridinoline, were used as markers of bone resorption and were validated by NMR spectroscopy and mass spectrometry [73]. Currently, there is no consensus if the 1660 and 1690 cm^{-1} ratio corresponds to collagen maturity or reflects the modification of the enzymatic cross-links (Table 2). The nonnegligible interference of the noncollagenous molecules, the different extinction coefficients of water and collagen, and the complex process of collagen maturation by enzymatic and nonenzymatic mechanisms impose uncertainty on the ratio measured. The spatial variation of collagen maturity in terms of the ratio of mature, nonreducible, pyridinoline (PYD) (or deoxypyridinoline, d-Pyr) to immature dehydro-dihydroxylysinonorleucine (deH-DHLNL) using FTIR

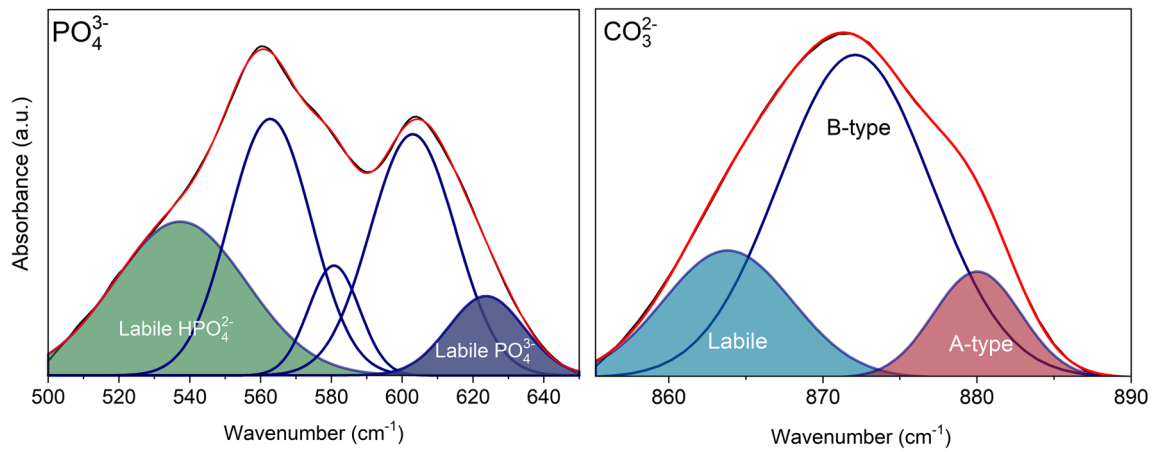

Fig. 2 Typical example of band deconvolution of the PO_4^{3-} v_4 and CO_3^{2-} v_2 FTIR peaks to the respective moiety sub-bands

Table 2 Peak ratio parameters used in the FTIR analysis of bone moieties [58–64]

Parameter	Methodology and tentative peaks position (small deviations are normal due to instrumental and specimens variations)	Comments
Mineral to matrix ratio	Area of 900–1200 cm^{-1} phosphate band/area of amide I band (1600–1720 cm^{-1}) or area 500–650 cm^{-1} phosphate band[a])/area of amide I band (1600–1720 cm^{-1})	Measure of mineral per amount of collagen present Related to ash weight Reflects hyper- or hypo-mineralization (i.e., it is regarded as BMD approximation) Suggested as a surrogate of bending stiffness [65] Increases with age
Mineral maturity	Peak area or intensity ratio of sub-bands at 1030 cm^{-1} (stoichiometric apatites) and 1020 cm^{-1} (nonstoichiometric apatites) or 1030/1101 cm^{-1} or 604/563 cm^{-1} *for crystallinity*: $FWHM^{-1}$ of the 604 cm^{-1} peak or sum of peak intensities at 604 and 563 cm^{-1} ($\nu_4(PO_4)$ vibrational mode) divided by the intensity of the valley between them (infrared splitting factor, IRSF) [66]	Often interrelated with "crystallinity"
Carbonate to mineral ratio	Area of 850–890 cm^{-1} carbonate band to phosphate bands	Increases with age Inverse linearly related to elastic modulus
Carbonate accumulation	Area of 850–890 cm^{-1} carbonate band to amide I band	Correlated to turnover rate, remodeling activity, and mineral dissolution Analysis can discriminate between type-A and type-B hydroxyapatite
Acid phosphate substitution	Peak area or intensity ratio of sub-bands at 1163 and 1028 or 957 cm^{-1} or intensity ratio of 540/563 cm^{-1}	Decreases with age Inversely related to crystallinity
Collagen cross-links	Peak area or intensity ratio of sub-bands at 1660 cm^{-1} and 1690 cm^{-1} (or 1680 cm^{-1} for d-Pyr) of the amide I band	Often refers as "collagen maturity" Linearly correlated to crystallinity Still under investigation for the correct biological interpretation although widely used

[a] Curve fitting analysis of the ν_4 contour is preferable due to fewer sub-bands, lower absorption coefficient and saturation effects ([47]; [67])

(micro) spectroscopy was analyzed by comparing samples from bovine predentin and dentin, skin collagen, and human healthy femoral biopsy specimens [74]. On the other hand, Farlay et al. used lathyritic rats to demonstrate that the 1660/1690 cm^{-1} area ratio is specifically correlated to alterations in secondary structure of collagen related to the mineralization process instead of variations in the enzymatic cross-links [75]. Those results were confirmed by multivariate analysis of multispectral infrared images. Positive correlations were observed between both collagen maturity and mineral maturity (1660/1690 cm^{-1} and 1030/1110 cm^{-1} area ratio, respectively) although in that case, spectral sub-band decomposition was performed on fixed peak frequencies, instead of the usual second-derivative method, possibly introducing bias. Although collagen cross-link ratio is one major determinant of bone strength, the content and structure are also crucial for mechanical properties. Since the amide I band is a composite of molecular FTIR active groups (collagen, water molecules, and noncollagenous proteins), additional studies are carried out to confirm collagen state and integrity.

Preclinical and Clinical Applications

FTIR techniques applied on tissues are often characterized as clinical spectroscopy [76]. As previously discussed, a solid advantage of infrared spectroscopic methods is that they may reveal tissue abnormalities before they can be visually detected. Ergo, they can have momentous prognostic value by tracing early biochemical events that precede morphological abnormalities. However, specifically for bone research, the power of FTIR is anticipated in preclinical, ex vivo, studies because bone is not an exposed, directly palpable tissue, and therefore, it is not visible by optical or infrared methods. Therefore, excisional human bone biopsies are the main proxies for clinical applications especially when chemical and radiographic data are not diagnostic.

One of the advantages of the preclinical (animal) experiments is the ability to study a relatively standardized group of animals instead of a diverse group of patients. Furthermore, preclinical studies can help to investigate the etiology of the underlying bone pathology, the mechanisms of the associated disease, and the toxicological effects of proposed

interventions before clinical studies [77]. For example, BMD measurements of the lumbar spine following therapy ideally target the trabecula-rich vertebral body and ignore the contribution of cortical bone which is present but relatively insensitive to bone loss. In such cases, when trabecular cannot be discriminated from cortical bone, preclinical animal model is a suitable surrogate for the evaluation of compositional and mechanical properties possibly altered by a drug. Nevertheless, new therapies that have been characterized as successful in animal studies are often less effective in clinical trials. However, in a systematic review for the comparison of treatment effects between animal experiments and clinical trials [78], the controversial treatment of osteoporosis with bisphosphonates was the only analysis, among others irrelevant to bone tissue, that agreed between animal and clinical studies. Nevertheless, it is known that no animal model can accurately replicate the symptoms of spontaneous osteoporosis since, from mammalian species, only humans experience fractures during their normal life span. However, it was suggested that human osteoporosis can be reliably evaluated in carefully defined animal models [79].

Heterogeneity, Fragility, and Fracture Risk

Current clinical practice utilizes dual X-ray absorptiometry (DEXA) as the gold standard for assessing fracture risk. However, age was associated with 10-fold increase in fracture risk while entirely independent of BMD [80]. Loss of heterogeneity, as expressed by loss of collagen plasticity and increased osteon density, has been suggested to contribute to the increased bone microdamage, particularly with age [81]. Microcracks tend to avoid the osteons along the weak, noncollagenous cement lines at the border of the osteons [82]. The osteon density increases with age activating more cement lines where fatigue damage can form [83]. The heterogeneity of bone's compositional and/or mechanical properties may, or may not, contribute to fracture risk since a consensus for the positive (or negative) contribution has not yet emerged [84, 85]. Decreased bone heterogeneity is often negatively correlated to fracture toughness [86] while finite element analysis studies suggest that loss of heterogeneity and increased porosity trigger the age-related loss in bone toughness [87]. Still, size-dependent heterogeneity is expected to influence strength and fracture resistance [88]. At the atomic scale, low and nonhomogeneous 3D spatial distribution of calcium to phosphorus ratio (explored by dual-energy analysis (DEA) techniques, not traceable by FTIR spectroscopy) in rabbits' cortical bone samples with induced secondary osteoporosis was shown to be significantly different compared to Ca/P ratio of normal rabbit bone sections [89–91]. At larger length scales (nanometers), heterogeneity reflects organic–mineral interactions and the alterations in mineralized collagen fibrils and hydroxyapatite particles. Boskey et al. [92] examined ilial crest biopsies of 60 female patients with fractures and 60 age- and BMD-matched samples without fractures (total 120) and assessed using FTIR imaging, five bone quality variables (mineral to matrix ratio, carbonate to phosphate ratio, crystallinity, acid phosphate substitution, and collagen maturity), and their heterogeneity (defined as the linewidth at half-maximum of the image pixel distributions) pairing for age and BMD. Multivariate analyses suggested that decreased carbonate-to-phosphate ratio in both cancellous and cortical bone and increased collagen maturity heterogeneity for cancellous bone only were significant explanatory variables of fracture. In an earlier study performed with FTIR spectroscopic imaging [93], logistic regression analysis (with fracture as the dependent variable) was performed to a similar set of iliac crest biopsies from 54 women (32 with fractures, 22 without) to assess whether specific differences in spatially resolved bone composition (mineral content, mineral crystal size and perfection, and collagen maturity) contribute to fracture risk. The constructed model positively linked cortical and cancellous collagen maturity, cortical mineral/matrix ratio, and cancellous crystallinity with increased fracture risk while it showed a negative correlation between carbonate/mineral ratio and fracture risk. A follow-up FTIR imaging study with a subset of the same samples (21 biopsies positive to fractures and 12 negative) [94] showed that distributions of mineral and collagen properties differ between bones with and without fragility fractures independently of BMD. Moreover, the authors suggested that mean as well as low-tail distribution values of mineral to matrix ratio and collagen maturity were altered in patients with fragility fractures whereas newly formed tissue with imperfect crystallites and immature collagen cross-linking was an important characteristic of healthy, fracture-resistant bone. Decreased levels of heterogeneity were also noted in osteopenic patients [95]. Specifically, narrow spatial distributions of mineral to matrix ratio and carbonate to phosphate ratio in femoral neck sections from patients with hip fractures were observed. On the other hand, the heterogeneity of crystallinity, as measured by FTIR imaging, was increased in hip fractures compared to that of fracture-free cadaveric controls.

An animal model study with atomic force microscopy (AFM) and FTIR was recently conducted to investigate cancellous bone tissue (vertebral biopsies from ovariectomized sheep) composition at 50–100-nm resolution [96]. In that study, the collected spectra were described as "nanomechanical" because the absorption was proportional to the AFM cantilever oscillation, and novel compositional and structural changes in cancellous bone were found and compared to the standard FTIR imaging. Using IR spectroscopy and AFM (in separate experiments conducted with Wistar rats), it has been proposed that in early stages of osteoporosis, the hydration of hydroxyapatite crystals stimulates the swelling of collagen fibrils promoting the subsequent depression in the spatial arrangement of hydroxyapatite

nucleation sites [97] contrary to normal bone which typically has relatively regularly arranged grain spheres. The heterogeneity of the acid phosphate parameter was found to be significantly less in osteoporotic samples from an ovariectomized rat model of postmenopausal osteoporosis using FTIR [98]. Although changes in acid phosphate heterogeneity have not yet been observed in human osteoporotic bones, it is probably indicative of reduced new bone deposition in osteoporosis.

Osteoporosis

Mineral Composition

Osteoporosis is a systemic skeletal disorder characterized by deteriorating bone mass and microarchitecture leading to increased fracture risk and decreased quality of life [99, 100]. In osteoporosis, the resorptive activity of osteoclasts surpasses the formative activity of osteoblasts. Multiple combined factors increase the fracture risk of bone which can be divided into three general categories: mechanical loading, bone structure, and tissue material properties [101]. The latter can be extensively assessed by FTIR spectroscopy and imaging in order to investigate tissue alterations ex vivo. Osteoporotic tissues in humans [102] as well as animal models of osteoporosis [103] are characterized by decreased mineral to matrix ratio and thus by reduced mineral content. Moreover, both human and animal studies demonstrated that this decrease in osteoporotic bone is accompanied by an increase in crystallinity [104], and cortical bone from human osteoporotic iliac crest biopsies was found to be more crystalline than normal bone [102].

FTIR was able to detect spatial and temporal variation in bone properties at the surface of trabecular bone in high- and low-turnover osteoporosis human samples [105]. High-turnover samples (six biopsies) were characterized by increased resorptive surface, higher than normal numbers of osteoclasts, and increased or normal osteoblastic activity. On the other hand, low turnover (six biopsies) had lower than normal resorptive surface, decreased osteoclast number and osteoblastic activity. Low-turnover samples showed a slight increase in mineral to matrix ratio, carbonate accumulation, crystallinity, and acid phosphate content indicative of retarded, but existent, resorption and formation. Higher carbonate to phosphate ratio in iliac crest biopsies (statistically significant only for cortical bone) was reported from women who had sustained a fracture [106]. A tendency for a decreasing ratio at 2 mm away or further from the point of fracture was also observed. Thus, it remains unclear whether those carbonate ratio alterations are spatially limited to the fracture site. Further studies are needed to validate if the fractures, normally localized at the weakest location of the bone, are affected by spatially restricted changes in the carbonate sites of the bone apatite. This result was confirmed by FTIR spectroscopic studies where an increase of 11% in human cancellous bone fractures was observed in femoral neck [107]. Nevertheless, no significant increase for carbonate parameters was observed in iliac crest biopsies from high- and low-turnover osteoporosis [105]. Distribution of acid phosphate content along with carbonate parameters can be useful as biomarkers for characterizing (i) areas of reduced strength and (ii) the efficiency of pharmaceuticals for therapies of metabolic bone diseases, like osteoporosis, targeting mineral composition. Moreover, the variance of the mineral ions may also hint the importance of the collagenous matrix structure for bone fragility, suggesting that aging is crucial but not the only worth studying parameter in osteoporosis. When CO_3^{2-} and/or HPO_4^{2-} contents are high, A-type substitution is reduced. Acid phosphate content is indicative of apatite crystal size and perfection, and therefore denotes areas of new bone formation. Altered acid phosphate content has been related to alterations in bone strength [108]. For crystallinity, when iliac crest biopsies from patients with idiopathic juvenile osteoporosis were studied using FTIR imaging, crystallinity was not significantly different from juvenile controls; yet, acid phosphate substitution was increased in cancellous bones whereas carbonate to phosphate ratio was decreased [109]. That contradictory finding was explained by a net zero change in the overall crystallinity parameter by a simultaneous inversely related variation in acid phosphate substitution and carbonate to phosphate ratio.

In animal models, it was found that apatite crystal perfection increased collagen cross-linking and decreased mineral content which are time-dependent bone properties that play a major role in fragility [110]. Similarly to human biopsies, the most unstable parameter in osteoporotic animal samples appears to be the carbonate to mineral ratio (carbonate to phosphate ratio) and carbonate content. Although bone contains significantly less carbonate than phosphate, carbonate specific parameters are key variables for bone strength since they are indicative of turnover rate, remodeling activity, and mineral dissolution. Carbonate accumulation is an unstable parameter in many FTIR studies, and it either increases [111] or decreases [112–114]. Possibly, this discrepancy is due to the fact that this parameter refers to the total carbonate content neglecting the contribution of each type [67]. Specifically, an increase of the nonapatitic (labile) carbonate locations infers increased bone turnover rates even if the B-type/A-type content remains constant beyond a certain age [115]. In ovariectomized adult monkeys, the acid phosphate content was found to be elevated in the fracture prone animals [111]. Moreover, synchrotron FTIR studies on microdamaged bone of beagle dogs revealed increased content of acid phosphate ions at the sites of the damage [116]. Acid phosphate content also showed a statistical important increase in rabbit samples from an inflammation-mediated osteoporosis model [67]. This

can be explained by the replacement of PO_4^{3-} for HPO_4^{2-} ions in the osteoporotic bones and the creation of an anionic vacancy in the apatite crystal lattice, which is either compensated for by the removal of a Ca^{2+} cation or by CO_3^{2-} substitution in line with the increase of the highly reactive carbonate ions. Labile HPO_4^{2-} content was found to be inversely correlated with Ca^{2+} ions in the hydroxyapatite lattice in osteoporotic rabbits. After treatment of diseased rabbits with relatively high dose of calcium supplementation, increased carbonate content accompanied by decreased labile ion concentrations were found evincing stable apatitic environments [117].

Collagen Cross-linking

Collagen enzymatic and nonenzymatic cross-link formation has a strong effect on the mechanical properties of bone by affecting both mineralization process and microdamage formation. Reduced enzymatic cross-linking and/or increased nonenzymatic cross-links have been suggested as determinants of impaired bone mechanical properties in aging and osteoporosis [118]. Specifically, nonenzymatic cross-linking in mature cortical bone affects the quality of bone in human and animal models [119, 120]. The role of collagen in bone health has been studied extensively, and there is evidence that in postmenopausal osteoporosis, the relative amounts of mature and immature collagen cross-links contribute significantly to bone fragility due to alteration in bone tissue turnover rate [121]. Variance in collagen maturity and cross-linking properties are generally associated with bone mechanical properties and fracture resistance [122]. Using FTIR imaging, human fracture biopsies were compared with nonfracture biopsies and statistically significant differences were observed in cortical and cancellous bone for collagen maturity (higher mean values of PYD/deH-DHLNL cross-links) [93]. FTIR imaging of iliac crest biopsies from 14 individuals (10 male, 4 female) was used to assess the nonenzymatic cross-linking distribution in human osteoporotic trabecular bone before and after bisphosphonate treatment with third-generation bisphosphonates administered along with calcium and vitamin D supplementation [123]. The evaluation of nonenzymatic cross-link ratio (area ratio of 1678/1692 cm^{-1}) revealed no significant variation before and after bisphosphonate treatment. Nevertheless, the spatial distribution of the cross-links indicated that significant changes in collagen quality occur with tissue age. Similarly, FTIR assessment of iliac crest biopsies from fracture and nonfracture cohorts revealed that mean collagen maturity, in both cortical and trabecular bone, is associated with increased fragility and fracture risk. Low-tail values of collagen maturity distribution (immature collagen) is indicative of increased osteoblast activity (or decreased resorption) of new bone discriminating patients undergone fracture [94]. FTIR imaging analysis of the spatial distribution of the pyridinium/reducible collagen cross-link ratio between normal and osteoporotic sections from human iliac crest biopsies indicated differences at forming trabecular surfaces [124]. In three groups that were examined (female and male patients with high-turnover osteoporosis and low-turnover osteoporosis, and normal premenopausal women who had sustained spontaneous low-trauma fractures), a higher ratio of nonreducible to reducible collagen cross-links was found implying the critical role of abnormal collagen to bone fragility.

An increased collagen cross-link ratio in cortical bone of femoral midshaft of ovariectomized rabbits was also detected by Wen el al. [125] using FTIR analysis. The resulted decline in cortical bone strength was also confirmed by biomechanical tests. High collagen cross-links ratio was suggested to be the result of either abnormal collagen matrix or due to the possibility that the diseased bone matrix (e.g., with estrogen withdrawal or osteoporosis) matures at a faster rate than in normal bone. Possibly, it undergoes posttranslational modification because of a delay or alteration in mineralization.

Bisphosphonate Treatment

Spectroscopic techniques have the potential to assess the quality of healing tissues under medical treatment. An excellent review on pharmaceuticals that affect bone quality has been recently published [126]. In this section, we discuss FTIR studies on the effect of biphoshonates on osteoporotic bone tissue. Biphoshonates are the most widely prescribed antiresorptive drugs used for the treatment of osteoporosis and other diseases that are characterized by increased bone resorption. They play a key role in the management of postmenopausal osteoporosis since they increase areal BMD and decrease fracture risk. However, questions have arisen about the optimum duration of treatment and treatment holidays because long-term bisphosphonate administration has been associated with side effects mainly manifested as atypical femoral fractures (AFFs) [127]. As a result, bisphosphonates have the capacity to increase bone quantity, but their effects on bone quality are diverse. Although the incidence of side effects is relatively low, there is serious concern that prolonged osteoclast suppression may be deleterious as shown by the catastrophic nature of the fracture and the delayed healing. Long-term treatment with biphosphonates has been linked to molecular changes in mineral composition, collagen cross-linking, and diminished bone heterogeneity [128]. The pharmacological potency of bisphosphonates along with their speed in fracture reduction, skeletal uptake and distribution, bone affinity, and duration of action varies significantly. Moreover, data generated from direct comparisons from clinical trials are scarce [129]. Therefore, the study of specific bisphosphonate molecules along with their site-related modes of action have drawn significant attention by biospectroscopists in an effort to assess their effect on bone tissue hierarchical levels. As discussed, bisphosphonates promote osteoclast apoptosis

reducing osteoclastic activity and directly affect bone mineral content, crystallinity, and collagen cross-links.

In vitro FTIR studies evaluated the molecular interactions of risedronate with the apatitic surface of nanocrystalline apatites [130]. The latter can be used as bioactive biomaterials for orthopedic applications, since they contain an unstable hydrated layer structure acting as an ion reservoir for ion exchange or adsorption of organic pharmaceutical molecules [131]. Spectroscopic experiments revealed a strong interaction between risedronate and calcium at the surface which is attributed to the bonding between the pyridine nitrogen of risedronate and phosphate apatite groups. Transilial bone biopsies from a 3-year double-blind, randomized, placebo-controlled trial of alendronate in 447 healthy postmenopausal women were studied with FTIR imaging [132]. Alendronate treatment (10 mg kg^{-1}) resulted in elevated mineral to matrix ratio in cortical bone. Carbonate to phosphate ratio was decreased, and carbonate accumulation was not altered probably due to the increased phosphate content. Similarly, crystallinity and collagen cross-link ratio were not altered when compared to the control group in both cortical and cancellous bones. The heterogeneity of the bone tissue as calculated from the FWHM of pixel histograms was decreased for all the above parameters, perhaps reflecting the increased turnover of trabecular bone. A subsequent clinical study performed with micro-FTIR with the same type of biopsies and dose of alendronate but for longer treatment (6.4 ± 2.0 years) showed a significant increase in mineral maturity and a decrease in crystallinity [64]. That counter-intuitive result, i.e., the separation of crystallinity and mineral maturity, was also reported in women treated with zoledronate for 3 years [133] assessed by vibrational spectroscopy (Raman). The effect was accompanied by greater carbonate substitution. Longer-term administration of alendronate (8.0 ± 2.0 years) was assessed by micro-FTIR spectroscopy in an effort to investigate possible adverse effects of prolonged therapy on iliac cortical bone mineral and collagen quality [69]. Prolonged alendronate treatment was associated with higher collagen maturity and lower mineral crystallinity independently of the degree of mineralization although higher mean degree of cortical mineralization was observed in treated patients than that observed in untreated osteoporotic women. High degree of mineralization has been related to reduced heterogeneity of mineral content and remodeling activity possibly because, under bisphosphonate treatment, there is more time for bone to advance mineralization before being resorbed in the next remodeling cycle. Bone forming trabecular surfaces in 100 iliac crest biopsies from women with postmenopausal osteoporosis treated either with alendronate or risedronate for equivalent periods of 3–5 years revealed lower crystallinity and collagen cross-link ratio for risedronate than alendronate therapy although better suppression of bone turnover and increased BMD was observed in alendronate cases [134].

Compositional properties of proximal femoral cortical bone biopsies from bisphosphonate-treated patients with AFFs were compared with those from patients with typical osteoporotic fractures with and without bisphosphonate treatment using FTIR imaging [135]. Elevated mean mineralization was observed for patients with AFFs treated with bisphosphonates compared to those with typical fractures indicating greater tissue maturity arising from reduced remodeling. Moreover, cortical bone sections from patients with AFFs exhibited increased collagen maturity compared to those from patients without fractures. Similarly, significant compositional changes and decreased Haversian canal density in proximal femoral cortex were found between untreated osteoporotic and alendronate-treated (6.0 ± 1.6 years) osteoporotic individuals denoting the bisphosphonate influence on cortical osteoclasts [136]. Significantly higher mineral to matrix ratio than the osteoporosis and bisphosphonate-treated groups were found for young cortices. In addition, the carbonate to phosphate ratio was lower in osteoporosis and bisphosphonate-treated cases (albeit not significantly). Bisphosphonates, even at the low concentrations found in cortical bone, have been shown to increase the activity of osteoblasts and osteocytes despite the lower surface-to-volume ratio of cortical to trabecular bone [137]. It is therefore possible that the reduced bone turnover under bisphosphonate treatment promotes the reduction of the Haversian canal size and density while bone formation continues. Finally, a recent (preliminary) FTIR imaging study suggested that stopping the administration of alendronate for 5 years after a 5-year period of treatment would cause no major bone compositional changes [138]. Thirty-one iliac crest biopsies from two groups of postmenopausal women were evaluated for bone quality parameters (mineral to matrix ratio, carbonate to phosphate ratio, and collagen maturity), and no significant differences were found between continuously treated vs. group receiving alendronate for 10 years vs. group consisted of patients who received alendronate treatment for 5 years and no antiresorptive medication during the following 5 years. On the contrary, three additional parameters (cortical crystallinity, cortical acid phosphate heterogeneity, and trabecular crystallinity heterogeneity) were altered in a statistically significant manner, but these changes were characterized as relatively minor compared to the previous findings.

The effect of alendronate and risedronate was evaluated by FTIR imaging on an animal model of 30 healthy beagles treated daily for 1 year with these bisphosphonates [139]. No significant differences were detected between equivalent doses for risedronate and alendronate and for different doses of each drug. Mineral to matrix ratio was significantly different for areas in the endocortical third of the cortex while carbonate

to phosphate ratio and crystallinity did not yield any variation. Collagen cross-link ratio was significantly higher in bisphosphonate-treated groups compared to controls. However, in an older similar study with the same animal model, Burr et al. concluded that 1-year treatment with high doses of bisphosphonates bring no effect to the mineral crystals although bone remodeling was suppressed up to 90% [140]. Humeri of the same animals were used in a recent study to characterize alterations of the collagen and apatite mineral using synchrotron FTIR (increased brightness and signal to noise ratio) [141]. FTIR spectra analysis showed an increase in carbonate to phosphate ratio in the treated bone compared to control group as expected due to induced decrease in bone turnover and remodeling activity. No significant changes were detected in the degree of mineralization, crystallinity, and the enzymatic collagen cross-link ratio. In an ovine model of osteoporosis with dietary-induced metabolic acidosis, treatment with zoledronate increased mineral to matrix ratio throughout trabeculae but did not alter the collagen cross-linking network or the crystallinity [142].

Conclusion

FTIR spectroscopy (and related FTIR modalities) has great potential as a diagnostic tool for the investigation of diseased bone biopsies and for the ex vivo monitoring of treated bones with therapeutic agents. Alterations in the chemical composition of bone mineral and matrix can be simultaneously probed by FTIR spectroscopy in both qualitative and quantitative manner. Bone quality is an umbrella term that describes a set of intrinsic determinants which define the interactions of bone constituents at multiple hierarchical levels and thus bone strength and fracture toughness. Fracture risk is not solely dependent on BMD while the assessment of the structural and material properties of bone is central to better address tissue fragility. Understanding which parameters influence bone quality and how these are modified by aging, disease, and pharmaceuticals should lead to improved diagnosis and treatment of osteoporosis. Besides, assessment of bone quality parameters by FTIR techniques can provide insight on how antiresorptive drugs may disturb bone composition through microstructural deterioration.

Compliance with Ethical Standards

Conflict of Interest The authors declare that they have no conflict of interest.

Ethical Approval This article does not contain any studies with human participants or animals performed by any of the authors.

Informed Consent Not applicable.

References

1. Rabar S, Lau R, O'Flynn N, Li L, Barry P. Risk assessment of fragility fractures: summary of NICE guidance. BMJ. 2012;345(aug08 1):e3698.
2. Mccreadie BR, Goldstein SA. Biomechanics of fracture: is bone mineral density sufficient to assess risk? J Bone Miner Res. 2000;15(12):2305–8.
3. Patel AA, Ramanathan R, Kuban J, Willis MH. Imaging findings and evaluation of metabolic bone disease. Adv Radiol. 2015;2015:812794.
4. Talari AC, Martinez MA, Movasaghi Z, Rehman S, Rehman IU. Advances in Fourier transform infrared (FTIR) spectroscopy of biological tissues. Appl Spectrosc Rev. 2017;52(5):456–506.
5. Old OJ, Fullwood LM, Scott R, Lloyd GR, Almond LM, Shepherd NA, et al. Vibrational spectroscopy for cancer diagnostics. Anal Methods. 2014;6(12):3901–17.
6. Wagermaier W, Klaushofer K, Fratzl P. Fragility of bone material controlled by internal interfaces. Calcif Tissue Int. 2015;97(3):201–12.
7. Liu Y, Luo D, Wang T. Hierarchical structures of bone and bioinspired bone tissue engineering. Small. 2016;12(34):4611–32.
8. Wegst UG, Bai H, Saiz E, Tomsia AP, Ritchie RO. Bioinspired structural materials. Nat Mater. 2015;14(1):23–36.
9. Sabet FA, Najafi AR, Hamed E, Jasiuk I. Modelling of bone fracture and strength at different length scales: a review. Interface Focus. 2016;6(1):20150055.
10. Milovanovic P, Potocnik J, Stoiljkovic M, Djonic D, Nikolic S, Neskovic O, et al. Nanostructure and mineral composition of trabecular bone in the lateral femoral neck: implications for bone fragility in elderly women. Acta Biomater. 2011;7(9):3446–51.
11. van der Harst MR, Brama PA, van de Lest CH, Kiers GH, DeGroot J, van Weeren PR. An integral biochemical analysis of the main constituents of articular cartilage, subchondral and trabecular bone. Osteoarthr Cartil. 2004;12(9):752–61.
12. Kourkoumelis N. Osteoporosis and strontium-substituted hydroxyapatites. Ann Transl Med. 2016;4:1.
13. Chai YC, Carlier A, Bolander J, Roberts SJ, Geris L, Schrooten J, et al. Current views on calcium phosphate osteogenicity and the translation into effective bone regeneration strategies. Acta Biomater. 2012;8(11):3876–87.
14. Hu YY, Rawal A, Schmidt-Rohr K. Strongly bound citrate stabilizes the apatite nanocrystals in bone. Proc Natl Acad Sci. 2010;107(52):22425–9.
15. Baig AA, Fox JL, Young RA, Wang Z, Hsu J, Higuchi WI, et al. Relationships among carbonated apatite solubility, crystallite size, and microstrain parameters. Calcif Tissue Int. 1999;64(5):437–49.
16. Milovanovic P, Potocnik J, Djonic D, Nikolic S, Zivkovic V, Djuric M, et al. Age-related deterioration in trabecular bone mechanical properties at material level: nanoindentation study of the femoral neck in women by using AFM. Exp Gerontol. 2012;47(2):154–9.
17. Miller LM, Little W, Schirmer A, Sheik F, Busa B, Judex S. Accretion of bone quantity and quality in the developing mouse skeleton. J Bone Miner Res. 2007;22(7):1037–45.
18. Belbachir K, Noreen R, Gouspillou G, Petibois C. Collagen types analysis and differentiation by FTIR spectroscopy. Anal Bioanal Chem. 2009;395(3):829–37.
19. Yamauchi M. Collagen: the major matrix molecule in mineralized tissues. In: Anderson JJB, Garner SC, editors. Calcium and phosphorus in health and disease. NY: CRC Press; 1996.
20. Chappard D, Baslé MF, Legrand E, Audran M. New laboratory tools in the assessment of bone quality. Osteoporos Int. 2011;22(8):2225–40.

21. Landis WJ, Silver FH. Mineral deposition in the extracellular matrices of vertebrate tissues: identification of possible apatite nucleation sites on type I collagen. Cells Tissues Organs. 2009;189(1–4):20–4.
22. Boskey AL. Matrix proteins and mineralization: an overview. Connect Tissue Res. 1996;35(1–4):357–63.
23. Young MF. Bone matrix proteins: their function, regulation, and relationship to osteoporosis. Osteoporos Int. 2003;14(3):35–42.
24. Kourkoumelis N, Tzaphlidou M. Spectroscopic assessment of normal cortical bone: differences in relation to bone site and sex. Sci World J. 2010;10:402–12.
25. Hunt HB, Donnelly E. Bone quality assessment techniques: geometric, compositional, and mechanical characterization from macroscale to nanoscale. Clin Rev Bone Miner Metab. 2016;14(3):133–49.
26. Small RE. Uses and limitations of bone mineral density measurements in the management of osteoporosis. Medscape Gen Med. 2005;7(2):3.
27. Kanis JA. Assessment of fracture risk and its application to screening for postmenopausal osteoporosis: synopsis of a WHO report. Osteoporos Int. 1994;4(6):368–81.
28. Schuit SC, Van der Klift M, Weel AE, De Laet CE, Burger H, Seeman E, et al. Fracture incidence and association with bone mineral density in elderly men and women: the Rotterdam study. Bone. 2004;34(1):195–202.
29. Bouxsein ML. Bone quality: where do we go from here? Osteoporos Int. 2003;14(5):118–27.
30. Bouxsein ML, Seeman E. Quantifying the material and structural determinants of bone strength. Best Pract Res Clin Rheumatol. 2009;23(6):741–53.
31. Felsenberg D, Boonen S. The bone quality framework: determinants of bone strength and their interrelationships, and implications for osteoporosis management. Clin Ther. 2005;27(1):1–11.
32. Seeman E, Delmas PD. Bone quality—the material and structural basis of bone strength and fragility. N Engl J Med. 2006;354(21):2250–61.
33. Kourkoumelis N. Spectroscopy for biosciences. Contemp Phys. 2015;56(4):480–2.
34. Barth A. Infrared spectroscopy of proteins. Biochim Biophys Acta (BBA)-Bioenergetics. 2007;1767(9):1073–101.
35. Steiner G, Koch E. Trends in Fourier transform infrared spectroscopic imaging. Anal Bioanal Chem. 2009;394(3):671–8.
36. Cheng JX, Xie XS. Vibrational spectroscopic imaging of living systems: an emerging platform for biology and medicine. Science. 2015;350(6264):aaa8870.
37. Lopes CD, Limirio PH, Novais VR, Dechichi P. Fourier transform infrared spectroscopy (FTIR) application chemical characterization of enamel, dentin and bone. Appl Spectrosc Rev. 2018;53(9):747–69.
38. Kazarian SG, Chan KA. ATR-FTIR spectroscopic imaging: recent advances and applications to biological systems. Analyst. 2013;138(7):1940–51.
39. Querido W, Ailavajhala R, Padalkar M, Pleshko N. Validated approaches for quantification of bone mineral crystallinity using transmission Fourier transform infrared (FT-IR), attenuated Total reflection (ATR) FT-IR, and Raman spectroscopy. Appl Spectrosc. 2018;72(11):1581–93.
40. Ellingham ST, Thompson TJ, Islam M. The effect of soft tissue on temperature estimation from burnt bone using Fourier transform infrared spectroscopy. J Forensic Sci. 2016;61(1):153–9.
41. Gu C, Katti DR, Katti KS. Photoacoustic FTIR spectroscopic study of undisturbed human cortical bone. Spectrochim Acta A Mol Biomol Spectrosc. 2013;103:25–37.
42. Wang X, Zhai M, Zhao Y, Yin J. A review of articular cartilage and osteoarthritis studies by Fourier transform infrared spectroscopic imaging. Ann Joint. 2018;3:9.
43. Movasaghi Z, Rehman S, ur Rehman DI. Fourier transform infrared (FTIR) spectroscopy of biological tissues. Appl Spectrosc Rev. 2008;43(2):134–79.
44. Petra M, Anastassopoulou J, Theologis T, Theophanides T. Synchrotron micro-FT-IR spectroscopic evaluation of normal paediatric human bone. J Mol Struct. 2005;733(1–3):101–10.
45. Mkukuma LD, Skakle JM, Gibson IR, Imrie CT, Aspden RM, Hukins DW. Effect of the proportion of organic material in bone on thermal decomposition of bone mineral: an investigation of a variety of bones from different species using thermogravimetric analysis coupled to mass spectrometry, high-temperature X-ray diffraction, and Fourier transform infrared spectroscopy. Calcif Tissue Int. 2004;75(4):321–8.
46. Combes C, Cazalbou S, Rey C. Apatite biominerals. Fortschr Mineral. 2016;6(2):34.
47. Rey C, Shimizu M, Collins B, Glimcher MJ. Resolution-enhanced Fourier transform infrared spectroscopy study of the environment of phosphate ions in the early deposits of a solid phase of calcium-phosphate in bone and enamel, and their evolution with age. I: investigations in the ν_4 PO_4 domain. Calcif Tissue Int. 1990;46(6):384–94.
48. Wilson RM, Elliott JC, Dowker SE, Smith RI. Rietveld structure refinement of precipitated carbonate apatite using neutron diffraction data. Biomaterials. 2004;25(11):2205–13.
49. Ivanova TI, Frank-Kamenetskaya OV, Kol'tsov AB, Ugolkov VL. Crystal structure of calcium-deficient carbonated hydroxyapatite. Thermal decomposition. J Solid State Chem. 2001;160(2):340–9.
50. Byrne HJ, Knief P, Keating ME, Bonnier F. Spectral pre and post processing for infrared and Raman spectroscopy of biological tissues and cells. Chem Soc Rev. 2016;45(7):1865–78.
51. Rinnan Å. Pre-processing in vibrational spectroscopy—when, why and how. Anal Methods. 2014;6(18):7124–9.
52. Lasch P. Spectral pre-processing for biomedical vibrational spectroscopy and microspectroscopic imaging. Chemom Intell Lab Syst. 2012;117:100–14.
53. Kourkoumelis N, Tzaphlidou M. Multivariate statistical evaluation of bone site and sex as parameters for the Fourier transform infrared spectroscopic study of normal bone. Spectroscopy. 2010;24(1–2):99–104.
54. Baker MJ, Trevisan J, Bassan P, Bhargava R, Butler HJ, Dorling KM, et al. Using Fourier transform IR spectroscopy to analyze biological materials. Nat Protoc. 2014;9(8):1771–91.
55. Petibois C, Desbat B. Clinical application of FTIR imaging: new reasons for hope. Trends Biotechnol. 2010;28(10):495–500.
56. Paschalis EP, Gamsjaeger S, Klaushofer K. Vibrational spectroscopic techniques to assess bone quality. Osteoporos Int. 2017;28(8):2275–91.
57. Paschalis EP, DiCarlo E, Betts F, Sherman P, Mendelsohn R, Boskey AL. FTIR microspectroscopic analysis of human osteonal bone. Calcif Tissue Int. 1996;59(6):480–7.
58. Boskey AL, Imbert L. Bone quality changes associated with aging and disease: a review. Ann N Y Acad Sci. 2017;1410(1):93–106.
59. Boskey A, Camacho NP. FT-IR imaging of native and tissue-engineered bone and cartilage. Biomaterials. 2007;28(15):2465–78.
60. Miller LM, Vairavamurthy V, Chance MR, Mendelsohn R, Paschalis EP, Betts F, et al. In situ analysis of mineral content and crystallinity in bone using infrared micro-spectroscopy of the ν_4 PO_4^{3-} vibration. Biochim Biophys Acta (BBA) Gen Subj. 2001;1527(1–2):11–9.
61. Isaksson H, Turunen MJ, Rieppo L, Saarakkala S, Tamminen IS, Rieppo J, et al. Infrared spectroscopy indicates altered bone turnover and remodeling activity in renal osteodystrophy. J Bone Miner Res. 2010;25(6):1360–6.
62. Gourion-Arsiquaud S, Burket JC, Havill LM, DiCarlo E, Doty SB, Mendelsohn R, et al. Spatial variation in osteonal bone

properties relative to tissue and animal age. J Bone Miner Res. 2009a;24(7):1271–81.
63. Blank RD, Baldini TH, Kaufman M, Bailey S, Gupta R, Yershov Y, et al. Spectroscopically determined collagen Pyr/deH-DHLNL cross-link ratio and crystallinity indices differ markedly in recombinant congenic mice with divergent calculated bone tissue strength. Connect Tissue Res. 2003;44(3–4):134–42.
64. Bala Y, Farlay D, Chapurlat R, Boivin G. Modifications of bone material properties in postmenopausal osteoporotic women long-term treated with alendronate. Eur J Endocrinol. 2011;165:647–55.
65. Donnelly E, Chen DX, Boskey AL, Baker SP, van der Meulen MC. Contribution of mineral to bone structural behavior and tissue mechanical properties. Calcif Tissue Int. 2010;87(5):450–60.
66. Dal Sasso G, Asscher Y, Angelini I, Nodari L, Artioli G. A universal curve of apatite crystallinity for the assessment of bone integrity and preservation. Sci Rep. 2018;8(1):12025.
67. Kourkoumelis N, Lani A, Tzaphlidou M. Infrared spectroscopic assessment of the inflammation-mediated osteoporosis (IMO) model applied to rabbit bone. J Biol Phys. 2012;38(4):623–35.
68. Farlay D, Panczer G, Rey C, Delmas PD, Boivin G. Mineral maturity and crystallinity index are distinct characteristics of bone mineral. J Bone Miner Metab. 2010;28(4):433–45.
69. Bala Y, Depalle B, Farlay D, Douillard T, Meille S, Follet H, et al. Bone micromechanical properties are compromised during long-term alendronate therapy independently of mineralization. J Bone Miner Res. 2012;27(4):825–34.
70. Yamauchi M, Young DR, Chandler GS, Mechanic GL. Cross-linking and new bone collagen synthesis in immobilized and recovering primate osteoporosis. Bone. 1988;9(6):415–8.
71. Banse X, Sims TJ, Bailey AJ. Mechanical properties of adult vertebral cancellous bone: correlation with collagen intermolecular cross-links. J Bone Miner Res. 2002;17(9):1621–8.
72. Ritchie RO. The conflicts between strength and toughness. Nat Mater. 2011;10(11):817–22.
73. Robins SP, Duncan A, Wilson N, Evans BJ. Standardization of pyridinium crosslinks, pyridinoline and deoxypyridinoline, for use as biochemical markers of collagen degradation. Clin Chem. 1996;42(10):1621–6.
74. Paschalis EP, Gamsjaeger S, Tatakis DN, Hassler N, Robins SP, Klaushofer K. Fourier transform infrared spectroscopic characterization of mineralizing type I collagen enzymatic trivalent cross-links. Calcif Tissue Int. 2015;96(1):18–29.
75. Farlay D, Duclos ME, Gineyts E, Bertholon C, Viguet-Carrin S, Nallala J, et al. The ratio 1660/1690 cm^{-1} measured by infrared microspectroscopy is not specific of enzymatic collagen cross-links in bone tissue. PLoS One. 2011;6(12):e28736.
76. Goodacre R, Sergo V, Barr H, Sammon C, Schultz ZD, Baker MJ, et al. Clinical Spectroscopy: general discussion. Faraday Discuss. 2016;187:429–60.
77. Hooijmans CR, Ritskes-Hoitinga M. Progress in using systematic reviews of animal studies to improve translational research. PLoS Med. 2013;10(7):e1001482.
78. Perel P, Roberts I, Sena E, Wheble P, Briscoe C, Sandercock P, et al. Comparison of treatment effects between animal experiments and clinical trials: systematic review. BMJ. 2007;334(7586):197.
79. Bonjour JP, Ammann P, Rizzoli R. Importance of preclinical studies in the development of drugs for treatment of osteoporosis: a review related to the 1998 WHO guidelines. Osteoporos Int. 1999;9(5):379–93.
80. Hui SL, Slemenda CW, Johnston CC. Age and bone mass as predictors of fracture in a prospective study. J Clin Invest. 1988;81(6):1804–9.
81. Acevedo C, Stadelmann VA, Pioletti DP, Alliston T, Ritchie RO. Fatigue as the missing link between bone fragility and fracture. Nat Biomed Eng. 2018;2(2):62–71.
82. Gupta HS, Zioupos P. Fracture of bone tissue: the 'hows' and the 'whys'. Med Eng Phys. 2008;30(10):1209–26.
83. Zimmermann EA, Schaible E, Bale H, Barth HD, Tang SY, Reichert P, et al. Age-related changes in the plasticity and toughness of human cortical bone at multiple length scales. Proc Natl Acad Sci. 2011;108(35):14416–21.
84. Nyman JS, Granke M, Singleton RC, Pharr GM. Tissue-level mechanical properties of bone contributing to fracture risk. Curr Osteoporos Rep. 2016;14(4):138–50.
85. Currey J. Structural heterogeneity in bone: good or bad? J Musculoskelet Nueronal Interact. 2005;5(4):317.
86. Makowski AJ, Granke M, Uppuganti S, Mahadevan-Jansen A, Nyman JS. Bone tissue heterogeneity is associated with fracture toughness: a polarization Raman spectroscopy study. In SPIE BiOS. International Society for Optics and Photonics. SPIE Proc. 2015;9303:341.
87. Besdo S, Vashishth D. Extended finite element models of introcortical porosity and heterogeneity in cortical bone. Comput Mater Sci. 2012;64:301–5.
88. Yao H, Dao M, Carnelli D, Tai K, Ortiz C. Size-dependent heterogeneity benefits the mechanical performance of bone. J Mech Phys Solids. 2011;59(1):64–74.
89. Hadjipanteli A, Kourkoumelis N, Fromme P, Olivo A, Huang J, Speller R. A new technique for the assessment of the 3D spatial distribution of the calcium/phosphorus ratio in bone apatite. Physiol Meas. 2013;34(11):1399–410.
90. Hadjipanteli A, Kourkoumelis N, Speller R. Evaluation of CT-DEA performance on ca/P ratio assessment in bone apatite using EDX. X-Ray Spectrom. 2014;43(5):286–91.
91. Hadjipanteli A, Kourkoumelis N, Fromme P, Huang J, Speller RD. Evaluation of the 3D spatial distribution of the calcium/phosphorus ratio in bone using computed-tomography dual-energy analysis. Phys Med. 2016;32(1):162–8.
92. Boskey AL, Donnelly E, Boskey E, Spevak L, Ma Y, Zhang W, et al. Examining the relationships between bone tissue composition, compositional heterogeneity, and fragility fracture: a matched case-controlled FTIRI study. J Bone Miner Res. 2016;31(5):1070–81.
93. Gourion-Arsiquaud S, Faibish D, Myers E, Spevak L, Compston J, Hodsman A, et al. Use of FTIR spectroscopic imaging to identify parameters associated with fragility fracture. J Bone Miner Res. 2009;24(9):1565–71.
94. Wang ZX, Lloyd AA, Burket JC, Gourion-Arsiquaud S, Donnelly E. Altered distributions of bone tissue mineral and collagen properties in women with fragility fractures. Bone. 2016;84:237–44.
95. Gourion-Arsiquaud S, Lukashova L, Power J, Loveridge N, Reeve J, Boskey AL. Fourier transform infrared imaging of femoral neck bone: reduced heterogeneity of mineral-to-matrix and carbonate-to-phosphate and more variable crystallinity in treatment-naive fracture cases compared with fracture-free controls. J Bone Miner Res. 2013;28(1):150–61.
96. Imbert L, Gourion-Arsiquaud S, Villarreal-Ramirez E, Spevak L, Taleb H, van der Meulen MCH, et al. Dynamic structure and composition of bone investigated by nanoscale infrared spectroscopy. PLoS One. 2018;13(9):e0202833.
97. Gaidash AA, Sinitsa LN, Babenko OA, Lugovskoy AA. Nanoporous structure of bone matrix at osteoporosis from data of atomic force microscopy and IR spectroscopy. J Osteoporos. 2011;2011:1–7.
98. Mathavan N, Turunen MJ, Tägil M, Isaksson H. Characterising bone material composition and structure in the ovariectomized (OVX) rat model of osteoporosis. Calcif Tissue Int. 2015;97(2):134–44.
99. Rachner TD, Khosla S, Hofbauer LC. Osteoporosis: now and the future. Lancet. 2011;377(9773):1276–87.

100. Kourkoumelis N, Balatsoukas I, Tzaphlidou M. Ca/P concentration ratio at different sites of normal and osteoporotic rabbit bones evaluated by Auger and energy dispersive X-ray spectroscopy. J Biol Phys. 2012;38(2):279–91.
101. Burr DB, Forwood MR, Fyhrie DP, Martin RB, Schaffler MB, Turner CH. Bone microdamage and skeletal fragility in osteoporotic and stress fractures. J Bone Miner Res. 1997;12(1):6–15.
102. Paschalis EP, Betts F, DiCarlo E, Mendelsohn R, Boskey AL. FTIR microspectroscopic analysis of human iliac crest biopsies from untreated osteoporotic bone. Calcif Tissue Int. 1997;61(6):487–92.
103. Gadeleta SJ, Boskey AL, Paschalis E, Carlson C, Menschik F, Baldini T, et al. A physical, chemical, and mechanical study of lumbar vertebrae from normal, ovariectomized, and nandrolone decanoate-treated cynomolgus monkeys (Macaca fascicularis). Bone. 2000;27(4):541–50.
104. Faibish D, Ott SM, Boskey AL. Mineral changes in osteoporosis a review. Clin Orthop Relat Res. 2006;443:28–38.
105. Boskey AL, DiCarlo E, Paschalis E, West P, Mendelsohn R. Comparison of mineral quality and quantity in iliac crest biopsies from high-and low-turnover osteoporosis: an FT-IR microspectroscopic investigation. Osteoporos Int. 2005;16(12):2031–8.
106. McCreadie BR, Morris MD, Chen TC, Rao DS, Finney WF, Widjaja E, et al. Bone tissue compositional differences in women with and without osteoporotic fracture. Bone. 2006;39(6):1190–5.
107. Greenwood C, Clement J, Dicken A, Evans JP, Lyburn I, Martin RM, et al. Towards new material biomarkers for fracture risk. Bone. 2016;93:55–63.
108. Spevak L, Flach CR, Hunter T, Mendelsohn R, Boskey A. Fourier transform infrared spectroscopic imaging parameters describing acid phosphate substitution in biologic hydroxyapatite. Calcif Tissue Int. 2013;92(5):418–28.
109. Garcia I, Chiodo V, Ma Y, Boskey A. Evidence of altered matrix composition in iliac crest biopsies from patients with idiopathic juvenile osteoporosis. Connect Tissue Res. 2016;57(1):28–37.
110. Miller LM, Novatt JT, Hamerman D, Carlson CS. Alterations in mineral composition observed in osteoarthritic joints of cynomolgus monkeys. Bone. 2004;35(2):498–506.
111. Huang RY, Miller LM, Carlson CS, Chance MR. Characterization of bone mineral composition in the proximal tibia of cynomolgus monkeys: effect of ovariectomy and nandrolone decanoate treatment. Bone. 2002;30(3):492–7.
112. Bohic S, Rey C, Legrand A, Sfihi H, Rohanizadeh R, Martel C, et al. Characterization of the trabecular rat bone mineral: effect of ovariectomy and bisphosphonate treatment. Bone. 2000;26(4):341–8.
113. Ouyang H, Sherman PJ, Paschalis EP, Boskey AL, Mendelsohn R. Fourier transform infrared microscopic imaging: effects of estrogen and estrogen deficiency on fracture healing in rat femurs. Appl Spectrosc. 2004;58(1):1–9.
114. Huang RY, Miller LM, Carlson CS, Chance MR. In situ chemistry of osteoporosis revealed by synchrotron infrared microspectroscopy. Bone. 2003;33(4):514–21.
115. Akkus O, Adar F, Schaffler MB. Age-related changes in physicochemical properties of mineral crystals are related to impaired mechanical function of cortical bone. Bone. 2004;34(3):443–53.
116. Ruppel ME, Burr DB, Miller LM. Chemical makeup of microdamaged bone differs from undamaged bone. Bone. 2006;39(2):318–24.
117. Lani A, Kourkoumelis N, Baliouskas G, Tzaphlidou M. The effect of calcium and vitamin D supplementation on osteoporotic rabbit bones studied by vibrational spectroscopy. J Biol Phys. 2014;40(4):401–12.
118. Saito M, Marumo KM. Collagen cross-links as a determinant of bone quality: a possible explanation for bone fragility in aging, osteoporosis, and diabetes mellitus. Osteoporos Int. 2010;21(2):195–214.
119. SY T, Vashishth D. The relative contributions of non-enzymatic glycation and cortical porosity on the fracture toughness of aging bone. J Biomech. 2011;44(2):330–6.
120. Siegmund T, Allen MR, Burr DB. Failure of mineralized collagen fibrils: modeling the role of collagen cross-linking. J Biomech. 2008;41(7):1427–35.
121. Viguet-Carrin S, Garnero P, Delmas PD. The role of collagen in bone strength. Osteoporos Int. 2006;17(3):319–36.
122. Vashishth D. The role of the collagen matrix in skeletal fragility. Curr Osteoporos Rep. 2007;5(2):62–6.
123. Schmidt FN, Zimmermann EA, Campbell GM, Sroga GE, Püschel K, Amling M, et al. Assessment of collagen quality associated with non-enzymatic cross-links in human bone using Fourier-transform infrared imaging. Bone. 2017;97:243–51.
124. Paschalis EP, Shane E, Lyritis G, Skarantavos G, Mendelsohn R, Boskey AL. Bone fragility and collagen cross-links. J Bone Miner Res. 2004;19(12):2000–4.
125. Wen XX, Wang FQ, Xu C, Wu ZX, Zhang Y, Feng YF, et al. Time related changes of mineral and collagen and their roles in cortical bone mechanics of ovariectomized rabbits. PLoS One. 2015;10(6):e0127973.
126. Imbert L, Boskey A. Effects of drugs on bone quality. Clin Rev Bone Miner Metab. 2016;14(3):167–96.
127. Black DM, Abrahamsen B, Bouxsein ML, Einhorn T, Napoli N. Atypical femur fractures—review of epidemiology, relationship to bisphosphonates, prevention and clinical management. Endocr Rev. 2018; https://doi.org/10.1210/er.2018-00001.
128. Ettinger B, Burr DB, Ritchie RO. Proposed pathogenesis for atypical femoral fractures: lessons from materials research. Bone. 2013;55(2):495–500.
129. Russell RG, Watts NB, Ebetino FH, Rogers MJ. Mechanisms of action of bisphosphonates: similarities and differences and their potential influence on clinical efficacy. Osteoporos Int. 2008;19(6):733–59.
130. Errassifi F, Sarda S, Barroug A, Legrouri A, Sfihi H, Rey C. Infrared, Raman and NMR investigations of risedronate adsorption on nanocrystalline apatites. J Colloid Interface Sci. 2014;420:101–11.
131. Rey C, Combes C, Drouet C, Sfihi H, Barroug A. Physicochemical properties of nanocrystalline apatites: implications for biominerals and biomaterials. Mater Sci Eng C. 2007;27(2):198–205.
132. Boskey AL, Spevak L, Weinstein RS. Spectroscopic markers of bone quality in alendronate-treated postmenopausal women. Osteoporos Int. 2009;20(5):793–800.
133. Gamsjaeger S, Buchinger B, Zwettler E, Recker R, Black D, Gasser JA, et al. Bone material properties in actively bone-forming trabeculae in postmenopausal women with osteoporosis after three years of treatment with once-yearly zoledronic acid. J Bone Miner Res. 2011;26(1):12–8.
134. Hofstetter B, Gamsjaeger S, Phipps RJ, Recker RR, Ebetino FH, Klaushofer K, et al. Effects of alendronate and risedronate on bone material properties in actively forming trabecular bone surfaces. J Bone Miner Res. 2012;27(5):995–1003.
135. Lloyd AA, Gludovatz B, Riedel C, Luengo EA, Saiyed R, Marty E, et al. Atypical fracture with long-term bisphosphonate therapy is associated with altered cortical composition and reduced fracture resistance. Proc Natl Acad Sci. 2017;114(33):8722–7.
136. Milovanovic P, Zimmermann EA, Riedel C, vom Scheidt A, Herzog L, Krause M, et al. Multi-level characterization of human femoral cortices and their underlying osteocyte network reveal trends in quality of young, aged, osteoporotic and antiresorptive-treated bone. Biomaterials. 2015;45:46–55.
137. Plotkin LI, Lezcano V, Thostenson J, Weinstein RS, Manolagas SC, Bellido T. Connexin 43 is required for the anti-apoptotic effect

of bisphosphonates on osteocytes and osteoblasts in vivo. J Bone Miner Res. 2008;23(11):1712–21.

138. Boskey AL, Spevak L, Ma Y, Wang H, Bauer DC, Black DM, et al. Insights into the bisphosphonate holiday: a preliminary FTIRI study. Osteoporos Int. 2018;29(3):699–705.
139. Gourion-Arsiquaud S, Allen MR, Burr DB, Vashishth D, Tang SY, Boskey AL. Bisphosphonate treatment modifies canine bone mineral and matrix properties and their heterogeneity. Bone. 2010;46(3):666–72.
140. Burr DB, Miller L, Grynpas M, Li J, Boyde A, Mashiba T, et al. Tissue mineralization is increased following 1-year treatment with high doses of bisphosphonates in dogs. Bone. 2003;33(6):960–9.
141. Acevedo C, Bale H, Gludovatz B, Wat A, Tang SY, Wang M, et al. Alendronate treatment alters bone tissues at multiple structural levels in healthy canine cortical bone. Bone. 2015;81:352–63.
142. Burket JC, Brooks DJ, MacLeay JM, Baker SP, Boskey AL, van der Meulen MC. Variations in nanomechanical properties and tissue composition within trabeculae from an ovine model of osteoporosis and treatment. Bone. 2013;52(1):326–36.